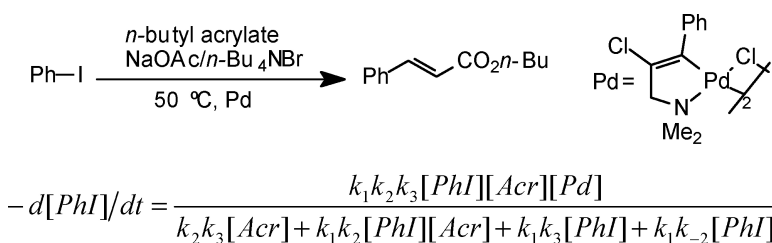


## Kinetics and Mechanistic Aspects of the Heck Reaction Promoted by a CN–Palladacycle

Crestina S. Consorti, Fabricio R. Flores, and Jairton Dupont

*J. Am. Chem. Soc.*, **2005**, 127 (34), 12054-12065 • DOI: 10.1021/ja051834q • Publication Date (Web): 06 August 2005

Downloaded from <http://pubs.acs.org> on March 25, 2009



### More About This Article

Additional resources and features associated with this article are available within the HTML version:

- Supporting Information
- Links to the 15 articles that cite this article, as of the time of this article download
- Access to high resolution figures
- Links to articles and content related to this article
- Copyright permission to reproduce figures and/or text from this article

[View the Full Text HTML](#)



## Kinetics and Mechanistic Aspects of the Heck Reaction Promoted by a CN–Palladacycle

Crestina S. Consorti, Fabrício R. Flores, and Jairton Dupont\*

Contribution from the Laboratory of Molecular Catalysis, Institute of Chemistry, UFRGS  
Avenida Bento Gonçalves, 9500 Porto Alegre 91501–970 RS Brazil

Received March 22, 2005; E-mail: dupont@iq.ufrgs.br

**Abstract:** In the Heck reaction between aryl halides and *n*-butyl acrylate, the palladacycle {Pd[ $\kappa^1$ -C,  $\kappa^1$ -N-C=(C<sub>6</sub>H<sub>5</sub>)C(Cl)CH<sub>2</sub>NMe<sub>2</sub>]( $\mu$ -Cl)}<sub>2</sub>, **1**, is merely a reservoir of the catalytically active Pd(0) species [**1**] (Pd colloids or highly active forms of low ligated Pd(0) species) that undergoes oxidative addition of the aryl halide on the surface with subsequent detachment, generating homogeneous Pd(II) species. The main catalytic cycle is initiated by oxidative addition of iodobenzene to [**1**], followed by the reversible coordination of the olefin to the oxidative addition product. All the unimolecular subsequent steps are indistinguishable kinetically and can be combined in a single step. This kinetic model predicts that a slight excess of alkene relative to iodobenzene leads to a rapid rise in the Pd(0) concentration while when using a slight excess of iodobenzene, relative to alkene, the oxidative addition product is the resting state of the catalytic cycle. Competitive experiments of various bromoarenes and iodoarenes with *n*-butyl acrylate catalyzed by **1** and CS, CP, and NCN palladacycles gave the same  $\rho$  value (2.4–2.5 for Ar–Br and 1.7–1.8 for Ar–I) for all palladacycles employed, indicating that they generate the same species in the oxidative addition step. The excellent fit of the slope with the  $\sigma_0$  Hammett parameter and the entropy of activation of  $-43 \pm 8 \text{ J mol}^{-1} \text{ K}^{-1}$  are consistent with an associative process involving the development of only a partial charge in the transition state for the oxidative step of iodobenzene.

### Introduction

Palladium-promoted C–C coupling reactions are one of the most important and investigated classes of organometallic reactions.<sup>1</sup> These catalytic processes possess several advantages when compared with more classical organic methods, such as their superb functional group tolerance, mild conditions employed, less waste, and sometimes fewer steps than the original stoichiometric routes. Among these catalytic processes, the formation of a C–C bond between alkenes and an aromatic ring—the Heck–Mizoroki reaction<sup>2,3</sup>—is finding increasing use for the industrial production of fine chemicals, such as monomers for coatings, pharmaceuticals, sunscreen agents, herbicides.<sup>4</sup> The coupling of alkenes with aryl halides can be accomplished by a plethora of palladium catalyst precursors under various reaction conditions. In fact, almost any molecular Pd(0) or Pd(II) catalyst precursor associated or not<sup>5</sup> with phosphorus, nitrogen, carbene and other ligands, colloids,<sup>6</sup> and supported<sup>7</sup> or heterogeneous<sup>8,9</sup> sources of palladium promotes the Heck–Mizoroki reaction involving aryl iodides and bromides. Among these catalytic processes, palladacycles including CP, CN, CS, PCP, SCS, NCN, SeCSe types<sup>10</sup> are one of the most investigated classes of catalyst precursors, in particular

due their facile synthesis, thermal stability, and possibility to modulate their steric and electronic properties.<sup>11</sup> Turnover numbers (moles of product/moles of Pd) ranging from 10<sup>4</sup> to 10<sup>6</sup> are easily achieved, depending on the nature of the base, solvent, temperature, and additive (usually N(*n*Bu)<sub>4</sub>Br salt, the so-called Jeffery conditions<sup>12</sup>) using these catalyst precursors.<sup>13</sup> However, these procedures still suffer limitations, such as not being applicable for less reactive and less expensive aryl

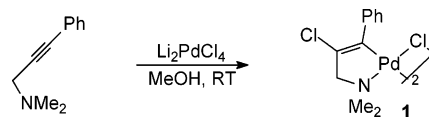
(1) (a) Negishi, E.; Ed. *Handbook of Organopalladium Chemistry for Organic Synthesis*; John Wiley & Sons: New York, 2002. (b) Bellina, F.; Carpita, A.; Rossi, R. *Synthesis* **2004**, 2419–2440. (c) Zapf, A.; Beller, M. *Chem. Commun.* **2005**, 431–440. (2) (a) Mizoroki, T.; Mori, K.; Ozaki, A. *Bull. Chem. Soc. Jpn.* **1971**, *44*, 581–581. (b) Heck, R. F.; Nolley, J. P. *J. Org. Chem.* **1972**, *37*, 2320–2322. (3) Beletskaya, I. P.; Cheprakov, A. V. *Chem. Rev.* **2000**, *100*, 3009–3066. (4) de Vries, J. G. *Can. J. Chem.-Rev. Can. Chim.* **2001**, *79*, 1086–1092.

(5) See for example: (a) Gruber, A. S.; Pozebon, D.; Monteiro, A. L.; Dupont, J. *Tetrahedron Lett.* **2001**, *42*, 7345–7348. (b) de Vries, A. H. M.; Parlevliet, F. J.; Schmieder-van de Vondervoort, L.; Mommers, J. H. M.; Henderickx, H. J. W.; Walet, M. A. M.; de Vries, J. G. *Adv. Synth. Catal.* **2002**, *344*, 996–1002. (c) de Vries, A. H. M.; Mulders, J. M. C. A.; Mommers, J. H. M.; Henderickx, H. J. W.; de Vries, J. G. *Org. Lett.* **2003**, *5*, 3285–3288. (d) Alimardanov, A.; de Vondervoort, L. S. V.; de Vries, A. H. M.; de Vries, J. G. *Adv. Synth. Catal.* **2004**, *346*, 1812–1817. (e) Reetz, M. T.; de Vries, J. G. *Chem. Commun.* **2004**, 1559–1563. (6) (a) Beller, M.; Fischer, H.; Kuhlein, K.; Reisinger, C. P.; Herrmann, W. A. *J. Organomet. Chem.* **1996**, *520*, 257–259. (b) Walter, J.; Heiermann, J.; Dyker, G.; Hara, S.; Shioyama, H. *J. Catal.* **2000**, *189*, 449–455. (c) Biffis, A.; Zecca, M.; Basato, M. *J. Mol. Catal. A-Chem.* **2001**, *173*, 249–274. (d) Kogan, V.; Aizenshtat, Z.; Popovitz-Biro, R.; Neumann, R. *Org. Lett.* **2002**, *4*, 3529–3532. (e) Moreno-Manas, M.; Pleixats, R. *Acc. Chem. Res.* **2003**, *36*, 638–643. (f) Mandal, S.; Roy, D.; Chaudhari, R. V.; Sastry, M. *Chem. Mater.* **2004**, *16*, 3714–3724. (g) Gniewek, A.; Trzeciak, A. M.; Ziolkowski, J. J.; Kepinski, L.; Wrzyszczyk, J.; Włodzimierz, T. *J. Catal.* **2005**, *229*, 332–343. (7) See, for example: (a) Djakovitch, L.; Heise, W.; Kohler, K. *J. Organomet. Chem.* **1999**, *584*, 16–26. (b) Bergbreiter, D. E.; Osburn, P. L.; Wilson, A.; Sink, E. M. *J. Am. Chem. Soc.* **2000**, *122*, 9058–9064. (c) Venkatesan, C.; Singh, A. P. *Catal. Lett.* **2003**, *88*, 193–197. (d) Corma, A.; Garcia, H.; Leyva, A. *Tetrahedron* **2004**, *60*, 8553–8560. (e) Venkatesan, C.; Singh, A. P. *J. Catal.* **2004**, *227*, 148–163. (f) Yu, K. Q.; Sommer, W.; Weck, M.; Jones, C. W. *J. Catal.* **2004**, *226*, 101–110. (g) Yu, K.; Sommer, W.; Richardson, J. M.; Weck, M.; Jones, C. W. *Adv. Synth. Catal.* **2005**, *347*, 161–171. (h) Bergbreiter, D. E.; Osburn, P. L.; Frels, J. D. *Adv. Synth. Catal.* **2005**, *347*, 172–184.

chlorides,<sup>14</sup> not being easily recyclable, and requiring high reaction temperatures,<sup>15</sup> thus limiting the scope of substrates that can be used, i.e., those that are thermally stable. It is evident that a detailed, intimate knowledge of the steps and the reaction mechanism involved could provide new and/or more improved procedures for these C–C coupling reactions.

It is now accepted that in most of the cases, the catalytically active species involved in these reactions are based on Pd(0) and that the reaction proceeds through a Pd(0)/Pd(II) catalytic cycle,<sup>16</sup> whatever the nature of the catalyst precursor (ionic, molecular, colloidal, supported or “heterogeneous”).<sup>17</sup> Although in some cases it was proposed that the Heck reaction can occur at the metal surfaces of the colloidal or heterogeneous palladium-based catalyst precursors,<sup>9</sup> most experimental evidence points to them serving as a reservoir of soluble catalytically active species.<sup>8</sup> Supported Pd(II) catalysts have apparently similar roles in these coupling reactions, i.e., they are actually reservoirs of soluble ill-defined forms of catalytically active Pd(0) species.<sup>7</sup> There are various indications that in the arylation of alkenes

**Scheme 1.** Chloropalladation of *N,N*-Dimethyl-1-phenylpropargylamine



promoted by palladacycles, they act as a reservoir of catalytically active Pd(0) species (closely akin to “ligandless” precursors<sup>5</sup>), but there is also the involvement of colloidal palladium.<sup>11d</sup> In this context, the question as to whether the reaction is promoted by the nanoparticles themselves or that they serve as a reservoir of soluble catalytically active Pd species still remains open. However, it is not a simple task to distinguish between so-called “homogeneous” and “heterogeneous” catalysts,<sup>18</sup> in particular in the reactions promoted by transition-metal compounds. Notwithstanding, there are now several approaches, such as poisoning experiments; intrinsic kinetics, related to the formation of the nanoparticles and with the catalytic reaction itself; and physical–chemical analysis (transmission electron microscopy, for instance) that can be used as probes to determine the nature of the “true” catalyst. Although some of these approaches have been used to probe the species involved in the Heck reaction promoted by palladacycles, only limited conclusions have appeared so far, most of them indicating that they are precatalysts of ill-defined Pd(0) catalytically active species.<sup>5c,15b,17d,19</sup> We have recently reported that the palladacycle **1** derived from the chloropalladation of *N,N*-dimethyl-1-phenylpropargylamine (Scheme 1) is an outstanding catalyst precursor for the coupling of aryl iodides and bromides, and these reactions can be conducted at room temperature.<sup>15b</sup> In this particular case, Hg poisoning experiments indicated the involvement of low-ligated Pd(0) as the catalytically active species. We have now employed several of the most used physical–chemical probes to determine not only the nature of the species involved in the Heck reaction promoted by palladacycle **1** but also the kinetics and mechanism of this process.

## Experimental Section

**General Methods.** All catalytic reactions were carried out under an argon or nitrogen atmosphere in an oven-dried resealable Schlenk tube. All substrates were purchased from Acros and used without further purification. *N,N*-dimethylacetamide was degassed and stored over molecular sieves. Molten *n*-Bu<sub>4</sub>Br was exposed to vacuum for 1 h prior to use. NMR spectra were recorded on a Varian Inova 300 MHz spectrometer. In situ time-resolved IR analysis were performed in a Bomem B-102 spectrometer adapted with an ATR probe Axiom Dipper 210 equipped with a ZnSe reflectance element. In situ time-resolved UV analyses were performed in a Varian Cary 50 spectrophotometer. Gas chromatography analyses were performed on a Hewlett-Packard-5890 gas chromatograph with a FID detector and 30 m DB17 capillary column. TEM and EDS analysis were performed in a JEOL-JEM 2010 electronic microscope (200 kV). The CN (**1**),<sup>20</sup> CP (**2**),<sup>21</sup> CS (**3**),<sup>22</sup> and

- (8) (a) Djakovitch, L.; Kohler, K. *J. Organomet. Chem.* **2000**, *606*, 101–107. (b) Zhao, F. Y.; Bhanage, B. M.; Shirai, M.; Arai, M. *Chem. Eur. J.* **2000**, *6*, 843–848. (c) Biffis, A.; Zecca, M.; Basato, M. *J. Mol. Catal. A-Chem.* **2001**, *173*, 249–274. (d) Biffis, A.; Zecca, M.; Basato, M. *Eur. J. Inorg. Chem.* **2001**, 1131–1133. (e) Kohler, K.; Wagner, M.; Djakovitch, L. *Catal. Today* **2001**, *66*, 105–114. (f) Zhao, F. Y.; Murakami, K.; Shirai, M.; Arai, M. *J. Catal.* **2000**, *194*, 479–483. (g) Kohler, K.; Heidenreich, R. G.; Krauter, J. G. E.; Pietsch, M. *Chem. Eur. J.* **2002**, *8*, 622–631. (h) Heidenreich, R. G.; Krauter, E. G. E.; Pietsch, J.; Kohler, K. *J. Mol. Catal. A-Chem.* **2002**, *182*, 499–509. (i) Prockl, S. S.; Kleist, W.; Gruber, M. A.; Kohler, K. *Angew. Chem., Int. Ed.* **2004**, *43*, 1881–1882.
- (9) (a) Choudary, B. M.; Madhi, S.; Chowdari, N. S.; Kantam, M. L.; Sreedhar, B. *J. Am. Chem. Soc.* **2002**, *124*, 14127–14136. (b) Dams, M.; Drijkoningen, L.; Pauwels, B.; Van Tendeloo, G.; De Vos, D. E.; Jacobs, P. A. *J. Catal.* **2002**, *209*, 225–236. (c) Corma, A.; Garcia, H.; Leyva, A.; Primo, A. *Appl. Catal. A-Gen.* **2004**, *257*, 77–83. (d) Choudary, B. M.; Madhi, S.; Kantam, M. L.; Sreedhar, B.; Iwasawa, I. *J. Am. Chem. Soc.* **2004**, *126*, 2292–2293.
- (10) See for example: (a) Beller, M.; Fischer, H.; Herrmann, W. A.; Ofele, K.; Brossmer, C. *Angew. Chem., Int. Ed. Engl.* **1995**, *34*, 1848–1849. (b) Ohff, M.; Ohff, A.; vander Boom, M. E.; Milstein, D. *J. Am. Chem. Soc.* **1997**, *119*, 11687–11688. (c) Albisson, D. A.; Bedford, R. B.; Scully, P. N. *Tetrahedron Lett.* **1998**, *39*, 9793–9796. (d) Shaw, B. L.; Perera, S. D.; Staley, E. A. *Chem. Commun.* **1998**, 1361–1362. (e) Ohff, M.; Ohff, A.; Milstein, D. *Chem. Commun.* **1999**, 357–358. (f) Bergbreiter, D. E.; Osburn, P. L.; Liu, Y. S. *J. Am. Chem. Soc.* **1999**, *121*, 9531–9538. (g) Gruber, A. S.; Zim, D.; Ebeling, G.; Monteiro, A. L.; Dupont, J. *Org. Lett.* **2000**, *2*, 1287–1290. (h) (g) Alonso, D. A.; Najera, C.; Pacheco, M. C. *Org. Lett.* **2000**, *2*, 1823–1826. (i) Rocaboy, C.; Gladysz, J. A. *Org. Lett.* **2002**, *4*, 1993–1996. (j) Yao, Q. W.; Kinney, E. P.; Zheng, C. *Org. Lett.* **2004**, *6*, 2997–2999.
- (11) (a) Herrmann, W. A.; Bohm, V. P. W.; Reisinger, C. P. *J. Organomet. Chem.* **1999**, *576*, 23–41. (b) Dupont, J.; Pfeffer, M.; Spencer, J. *Eur. J. Inorg. Chem.* **2001**, 1917–1927. (c) Bedford, R. B. *Chem. Commun.* **2003**, 1787–1796. (d) Beletskaya, I. P.; Cheprakov, A. V. *J. Organomet. Chem.* **2004**, *689*, 4055–4082. (e) Dupont, J.; Consorti, C. S.; Spencer, J. *Chem. Rev.* **2005**, *105*, 2427–2571.
- (12) (a) Jeffery, T.; Galland, J. C. *Tetrahedron Lett.* **1994**, *35*, 4103–4106. (b) Jeffery, T. *Tetrahedron*, **1996**, *52*, 10113–10130.
- (13) Farina, V. *Adv. Synth. Catal.* **2004**, *346*, 1553–1582.
- (14) Littke, A. F.; Fu, G. C. *Angew. Chem., Int. Ed.* **2002**, *41*, 4176–4211.
- (15) Only two examples of Heck coupling at room temperature have been reported so far: (a) Littke, A. F.; Fu, G. C. *J. Am. Chem. Soc.* **2001**, *123*, 6989–7000. (b) Consorti, C. S.; Zanini, M. L.; Leal, S.; Ebeling, G.; Dupont, J. *Org. Lett.* **2003**, *5*, 983–986.
- (16) See, for example: (a) Amatore, C.; Jutand, A. *J. Organomet. Chem.* **1999**, *576*, 254–278. (b) Amatore, C.; Jutand, A. *Acc. Chem. Res.* **2000**, *33*, 314–321. (c) Cruz, S. C.; Aarnoutse, P. J.; Rothenberg, G.; Westerhuis, J. A.; Smilde, A. K.; Blik, A. *Phys. Chem. Chem. Phys.* **2003**, *5*, 4455–4460. (d) Buback, M.; Perkovic, T.; Redlich, S.; de Meijere, A. *Eur. J. Org. Chem.* **2003**, 2375–2382 and references therein.
- (17) (a) Reetz, M. T.; Westermann, E.; Lohmer, R.; Lohmer, G. *Tetrahedron Lett.* **1998**, *39*, 8449–8452. (b) Reetz, M. T.; Westermann, E. *Angew. Chem., Int. Ed.* **2000**, *39*, 165–168. (c) de Vries, A. H. M.; Parlevliet, F. J.; Schmieder-van de Vondervoort, L.; Gommers, J. H. M.; Henderickx, H. J. W.; Walet, M. A. M.; de Vries, J. G. *Adv. Synth. Catal.* **2002**, *344*, 996–1002. (d) Rocaboy, C.; Gladysz, J. A. *New J. Chem.* **2003**, *27*, 39–49. (e) Tromp, M.; Sietsma, J. R. A.; van Bokhoven, J. A.; van Strijdonck, G. P. F.; van Haaren, R. J.; van der Eerden, A. M. J.; van Leeuwen, P. W. N. M.; Koningsberger, D. C. *Chem. Commun.* **2003**, 128–129. (f) Cassol, C. C.; Umpierre, A. P.; Machado, G.; Wolke, S. I.; Dupont, J. *J. Am. Chem. Soc.* **2005**, *127*, 3298–3299.
- (18) (a) Lin, Y.; Finke, R. G. *Inorg. Chem.* **1994**, *33*, 4891–4910. (b) Widegren, J. A.; Finke, R. G. *J. Mol. Catal. A-Chem.* **2003**, *198*, 317–341.
- (19) (a) Nowotny, M.; Hanefeld, U.; van Koningsveld, H.; Maschmeyer, T. *Chem. Commun.* **2000**, 1877–1878. (b) Beletskaya, I. P.; Kashin, A. N.; Karlstedt, N. B.; Mitin, A. V.; Cheprakov, A. V.; Kazanov, G. M. *J. Organomet. Chem.* **2001**, *622*, 89–96. (c) Bedford, R. B.; Cazin, C. S. J.; Hursthouse, M. B.; Light, M. E.; Pike, K. J.; Wimperis, S. *J. Organomet. Chem.* **2001**, *633*, 173–181. (d) Eberhard, M. R. *Org. Lett.* **2004**, *6*, 2125–2128. (e) Consorti, C. S.; Ebeling, G.; Flores, F. R.; Rominger, F.; Dupont, J. *Adv. Synth. Catal.* **2004**, *346*, 617–624.
- (20) Dupont, J.; Basso, N. R.; Meneghetti, M. R.; Konrath, R. A.; Burrow, R.; Horner, M. *Organometallics* **1997**, *16*, 2386–2391.

NCN (**4**)<sup>23</sup> palladacycles were synthesized according to known procedures. Dibenzobicyclo[*a,e*]cyclooctatetraene (DCT)<sup>24</sup> was synthesized starting from dibenzobicyclo[2.2.2]octatriene(dibenzobarrelene).<sup>25</sup>

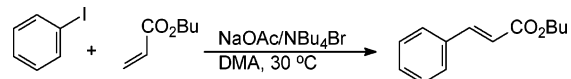
**In Situ UV Analysis.** A quartz cuvette (*b* = 1 cm) was charged with palladacycle **1** (2 mL of a  $4.76 \times 10^{-4}$  mol L<sup>-1</sup> DMA solution) and 1 mL of a DMA solution containing NaOAc (0.83 mmol/25 mL, 68 mg/25 mL), NBu<sub>4</sub>Br (0.12 mmol/25 mL, 38 mg/25 mL), and *n*-butyl acrylate (0.71 mmol/25 mL, 91 mg/25 mL). The reaction progress was followed by UV spectra.

**In situ ATR-IR Analysis.** A 50-mL glass reactor was evacuated and back-filled with argon and charged with sodium acetate (5.75 mmol, 460 mg) and tetrabutylammonium bromide (0.8 mmol, 256 mg). The flask was then connected to the ATR probe and then DMA (25 mL) was added, the temperature stabilized, and the background spectra acquired. *n*-Butyl acrylate (4.8 mmol, 687  $\mu$ L) and palladacycle **1** (500  $\mu$ L of a  $8 \times 10^{-3}$  mol L<sup>-1</sup> DMA solution,  $4 \times 10^{-3}$  mmol) were added to the reaction solution, and after a pretreatment time of 10 min, iodobenzene (4 mmol, 448  $\mu$ L) was added and the reaction monitored by IR. Iodobenzene and *trans*-*n*-butyl cinnamate concentrations, as a function of time, were obtained by integration of the 735 and 772 cm<sup>-1</sup> bands corrected by calibration curves. GC analyses of the reaction were performed at the end of the reaction and showed an excellent agreement with IR data (1–2% deviation).

**Typical Experiment for the Hammett Competition Reaction.** A 10-mL resealable Schlenk flask was evacuated and back-filled with argon and charged with sodium acetate (1.4 mmol, 112 mg) and tetrabutylammonium bromide (0.2 mmol, 64 mg). The flask was then evacuated and back-filled with argon and then *N,N*-dimethylacetamide (5 mL), *n*-butyl acrylate (10 mmol, 1.5 mL), methyl benzoate as internal standard (35 mg), 0.14 mmol of bromobenzene, and 0.14 mmol of one of the substrates 4-MeOPhBr, 4-MePhBr, 3-MePhBr, 4-CIPhBr, 4-ClPhBr, 3-ClPhBr, 4-CF<sub>3</sub>PhBr, 3-CF<sub>3</sub>PhBr, 4-NCPPhBr, 4-MeCOPhBr, or 4-NO<sub>2</sub>PhBr were added. After the addition of the palladacycle **1** in *N,N*-dimethylacetamide (42  $\mu$ L of a  $2.4 \times 10^{-5}$  mol L<sup>-1</sup> solution), the reaction mixture was stirred at 150 °C. The reaction was monitored by GC, and the initial relative rates were used to plot Hammett correlation. The competitive reactions were also performed with an excess of aryl halides (1.4 mmol of bromobenzene and 1.4 mmol of substituted bromoarene) relative to *n*-butyl acrylate (0.14 mmol) (see Supporting Information).

**Hg(0) Poisoning Test.** Two identical Heck experiments consisting of *n*-butyl acrylate (1.2 mmol, 172  $\mu$ L), iodobenzene (1 mmol, 112  $\mu$ L), 5 mL of *N,N*-dimethylacetamide, sodium acetate (1.4 mmol, 112 mg), tetrabutylammonium bromide (0.2 mmol, 64 mg), and palladacycle **1** in *N,N*-dimethylacetamide (42  $\mu$ L of a  $2.4 \times 10^{-3}$  mol L<sup>-1</sup> solution,  $10^{-3}$  mmol) were stirred at 80 °C. Aliquots were taken from both reactions and analyzed by GC. After 2 h, Hg (0.3 mmol, 60 mg) was added to one reaction vessel.

**Attachment of Halobenzoic Acids to Wang Resin.** Wang resin (2 g; OH loading: 1 mmol g<sup>-1</sup>, 2 mmol of OH) was suspended in 9:1 (v/v) CH<sub>2</sub>Cl<sub>2</sub>/DMF in a Schlenk flask. The halobenzoic acid (6 mmol), dicyclohexylcarbodiimide (1.24 g, 6 mmol), and 4-dimethylamino-pyridine (25 mg, 0.2 mmol) were added to the resin suspension, and the reaction mixture was refluxed for 4 h. The resin was collected in a filter funnel, washed with DMF (3 $\times$ ), H<sub>2</sub>O (3 $\times$ ), DMF (3 $\times$ ), CH<sub>2</sub>Cl<sub>2</sub> (3 $\times$ ), and MeOH (3 $\times$ ), and dried under vacuum. For an estimation of resin loading, 300 mg of Wang resin modified with the halobenzoic acid was suspended in trifluoroacetic acid:CH<sub>2</sub>Cl<sub>2</sub> 1:1 (v/v) and stirred

Scheme 2<sup>a</sup>

<sup>a</sup> Reaction conditions: DMA (5 mL), NaOAc (1.4 mmol), *n*-butyl acrylate (1.2 mmol) PhI (1 mmol), **1** ( $1.0 \times 10^{-3}$  mmol), and NBu<sub>4</sub>Br (0.2 mmol). Hg(0) (300:1 Hg: Pd) addition after 2 h.

for 2 h. The cleavage solution was dried under vacuum and the residual amount of free halobenzoic acid was employed to obtain the resin loading.

**Typical Experiment for the Heck Reaction of *n*-Butyl Acrylate with the Substrate Attached to the Wang Resin.** A 10-mL resealable Schlenk flask was evacuated and back-filled with argon and charged with sodium acetate (1.4 mmol, 112 mg), tetrabutylammonium bromide (0.2 mmol, 64 mg), and the Wang resin containing the attached 4-iodobenzoic acid (500 mg; I loading: 0.68 mmol g<sup>-1</sup>, 0.35 mmol of I), DMA (5 mL), *n*-butyl acrylate (0.5 mmol, 72  $\mu$ L), and palladacycle **1** (147  $\mu$ L of a  $2.4 \times 10^{-3}$  mol L<sup>-1</sup> DMA solution,  $3.5 \times 10^{-4}$  mmol). The reaction mixture was stirred at 30 °C for 24 h. The Wang resin was collected on a filter funnel, washed with DMF (3 $\times$ ), H<sub>2</sub>O (3 $\times$ ), DMF (3 $\times$ ), CH<sub>2</sub>Cl<sub>2</sub> (3 $\times$ ), and MeOH (3 $\times$ ), and dried under vacuum. The Wang resin was suspended in the cleavage solution (3 mL, trifluoroacetic acid:CH<sub>2</sub>Cl<sub>2</sub> 1:1 (v/v)) and stirred for 2 h. The cleavage solution was dried under vacuum and 1,3,5-tri-hydroxybenzene utilized as internal standard for <sup>1</sup>H NMR quantification of the Heck product. For Heck reactions with the acrylic resin, the cleavage of the Heck product was performed with dry methanol (4 mL) and LiBH<sub>4</sub> (200 mg) for 24 h. The reaction was quenched with the addition of wet methanol and the Heck product was quantified by <sup>1</sup>H NMR.

**DCT Inhibition Test.** Two identical Heck experiments consisting of *n*-butyl acrylate (1.2 mmol, 172  $\mu$ L), iodobenzene (1 mmol, 112  $\mu$ L), 5 mL of *N,N*-dimethylacetamide, sodium acetate (1.4 mmol, 112 mg), tetrabutylammonium bromide (0.2 mmol, 64 mg), and palladacycle **1** in dimethylacetamide (3.2 mg,  $10^{-2}$  mmol) were stirred at 30 °C. After 15 min, DCT ( $2 \times 10^{-2}$  mmol, 4 mg) was added to one reaction vessel. Aliquots were taken from both reactions and analyzed by GC.

## Results and Discussion

**Inhibition Tests.** As already pointed out, several known selective poisoning tests were applied to the catalytic systems in order to characterize homogeneous or heterogeneous components. One of the most popular is a Hg poisoning test that relies on the formation of amalgam with colloidal palladium, although poisoning of molecular Pd(0) cannot be excluded. Of note is that, as pointed by Whitesides,<sup>26</sup> a Hg poisoning test can confirm a homogeneous catalytic system but not a heterogeneous one. Mercury addition can even improve the catalytic activity of a heterogeneous hydrogenation reaction.<sup>27</sup> The Hg(0) poisoning test was performed in the Heck reaction of *n*-butyl acrylate and iodobenzene promoted by palladacycle **1** (Scheme 1). When compared to control reactions, a complete inhibition of the catalytic activity was observed after Hg (300 equiv) addition (Scheme 2).

This positive response to mercury poisoning test unfortunately cannot be taken as a confirmation of the presence of heterogeneous catalytically active palladium species in the Heck reaction but does confirm the intervention of Pd(0) species.

- (21) Herrmann, W. A.; Brossmer, C.; Ofele, K.; Reisinger, C. P.; Priemeier, T.; Beller, M.; Fischer, H. *Angew. Chem., Int. Ed. Engl.* **1995**, *34*, 1844–1848.  
 (22) Gruber, A. S.; Zim, D.; Ebeling, G.; Monteiro, A. L.; Dupont, J. *Org. Lett.* **2000**, *2*, 1287–1290.  
 (23) Consorti, C. S.; Ebeling, G.; Rodembusch, F.; Stefani, V.; Livotto, P. R.; Rominger, F.; Quina, F. H.; Yihwa, C.; Dupont, J. *Inorg. Chem.* **2004**, *43*, 530–536.  
 (24) Wong, H. N. C.; Sondheimer, F. *Tetrahedron* **1981**, *37*, 99–109.  
 (25) Rabideau, P. W. *OPPI Briefs* **1986**, *18*, 113–116.

- (26) Whitesides, G. M.; Hackett, M.; Brainard, R. L.; Lavalleye, J.-P. P. M.; Sowinski, A. F.; Izumi, A. N.; Moore, S. S.; Brown, D. W.; Staudt, E. M. *Organometallics* **1985**, *4*, 1819–1830.  
 (27) Georgiades, G. C.; Sermon, P. A. *J. Chem. Soc., Chem. Commun.* **1985**, 975–976.

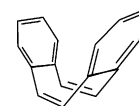
**Table 1.** Catalytic Activity of Palladacycle **1** with Polymer-Supported Substrates<sup>a</sup>

Entry	Substrate	substrate	[ArX]/[Pd]	Product	conditions	Yield <sup>b</sup>
1			1.0 x 10 <sup>2</sup>		30 °C, NaOAc/NBu <sub>4</sub> Br	85 <sup>c</sup>
2			1.0 x 10 <sup>3</sup>		80 °C, NaOAc/NBu <sub>4</sub> Br	90 <sup>c</sup>
3			1.0 x 10 <sup>5</sup>		130 °C, NaOAc/NBu <sub>4</sub> Br	100 <sup>c</sup>
4			1.0 x 10 <sup>6</sup>		130 °C, NaOAc/NBu <sub>4</sub> Br	75 <sup>c</sup>
5			1.0 x 10 <sup>3</sup>		120 °C, NaOAc/NBu <sub>4</sub> Br	90 <sup>c</sup>
6			1.0 x 10 <sup>3</sup>		120 °C, Na <sub>2</sub> CO <sub>3</sub>	24 <sup>c</sup>
7			1.0 x 10 <sup>3</sup>		120 °C, NaOAc	30 <sup>c</sup>
8			1.0 x 10 <sup>4</sup>		130 °C, NaOAc/NBu <sub>4</sub> Br	98 <sup>d</sup>
9			1.0 x 10 <sup>3</sup>		130 °C, NaOAc/NBu <sub>4</sub> Br	98 <sup>d</sup>
10		PhI	1.0 x 10 <sup>4</sup>		130 °C, NaOAc/NBu <sub>4</sub> Br	97 <sup>d</sup>

<sup>a</sup> Reaction conditions: 24 h, DMA (3 mL), resin (0.35 mmol), base (0.5 mmol), NBu<sub>4</sub>Br (0.1 mmol), *n*-butyl acrylate (0.5 mmol). <sup>b</sup> <sup>1</sup>H NMR yield after resin cleavage. <sup>c</sup> Cleavage with TFA/CH<sub>2</sub>Cl<sub>2</sub>. <sup>d</sup> Cleavage with LiBH<sub>4</sub> (internal standard 1,3,5-trihydroxybenzene).

The Collman test<sup>28</sup> is based on the ability of substrates attached to cross-linked polymers in distinguishing homogeneous or heterogeneous catalytically active species. Only soluble or highly solvated species are able to diffuse through the polymeric matrix, and as a consequence, only homogeneous catalytically active species are expected to show catalytic activity. The Collman test was successfully utilized with slight modifications recently in the Heck reaction of *n*-butyl acrylate and halobenzenes attached to poly(ethylene glycol) (three-phase test),<sup>29</sup> and no catalytic activity was observed with heterogeneous sources of palladium (Pd/alumina). However, the addition of a small quantity of a free substrate in the above catalytic system causes the insoluble substrate to be completely converted in the Heck product. This results strongly suggests the involvement of homogeneous catalytically active species in the Heck reaction even with traditional heterogeneous catalytic precursors: the oxidative addition of the free haloarene to the Pd(0) surface causes the release of Pd(II) species into the reaction solution, where the reaction proceeds according to the classical homogeneous mechanism and the substrate attached to the insoluble polymer can be converted.

The catalytic activity of the Heck reaction of iodo- and bromoarenes attached to cross-linked polystyrene promoted by palladacycle **1** is almost similar to those conducted with free substrates, and quantitative yields of the coupling products can be obtained after resin cleavage. Huge catalytic activities were

**Figure 1.** Dibenzo[*a,e*]cyclooctatetraene (DCT).

obtained ([ArX]/[Pd] = 1.0 × 10<sup>5</sup> (entries 3 and 6, Table 1), even without low concentrations of free substrate (three-phase test). These results strongly suggest that homogeneous catalytically active species are responsible for the catalytic activity observed.

In addition to showing that homogeneous palladium species were present with the Collmann test, we decided to run the test with the homogeneous species selective inhibitor dibenzo[*a,e*]cyclooctatetraene (DCT, Figure 1).<sup>30</sup> This poisoning test, known as Crabtree's test, is based on the ability of DCT to form stable and inert homogeneous complexes with platinum metals. The coordination of DCT to a heterogeneous surface is highly unfavorable, due to his rigid conformation. The irreversibility of the DCT–Pd complex formation and, as a consequence, the test validity depend on the reaction temperature. Since the Heck reaction promoted by palladacycle **1** can be performed at room temperature, the Crabtree test could be applied for the first time to the Heck reaction.

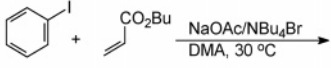
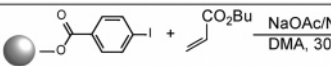
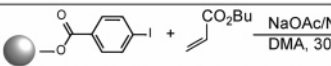
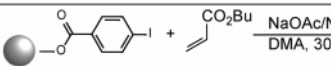
The general experimental protocol proposed by Crabtree includes the prior generation of the catalytically active species

(28) Collman, J. P.; Kosydar, K. M.; Bressan, M.; Lamanna, W.; Garrett, T. J. *Am. Chem. Soc.* **1984**, *106*, 2569–2579.

(29) Davies, I. W.; Matty, L.; Hughes, D. L.; Reider, P. J. *J. Am. Chem. Soc.* **2001**, *123*, 10139–10140.

(30) Anton, D. R.; Crabtree, R. H. *Organometallics* **1983**, *2*, 855–859.

**Table 2.** DCT Inhibition Tests<sup>a</sup>

Substrate	[DCT]/[Pd]	Relative yield (%)
	0	100 <sup>b</sup>
	2	40 <sup>b</sup>
	0	100 <sup>c</sup>
	2	50 <sup>c</sup>

<sup>a</sup> Reaction conditions: DMA (5 mL), NaOAc (1.4 mmol), olefin (1.2 mmol), ArX (1 mmol), **1** ( $1.0 \times 10^{-3}$  mmol), and NBu<sub>4</sub>Br (0.2 mmol). Reaction run with the Wang resin: DMA (3 mL), resin (0.35 mmol), base (0.5 mmol), NBu<sub>4</sub>Br (0.1 mmol), olefin (0.5 mmol). DCT (2:1 DCT: Pd) was added after 15 min. Relative reaction rate was obtained by comparison of conversions at 15 min and 24 h. <sup>b</sup> GC yield (internal standard methyl benzoate). <sup>c</sup> <sup>1</sup>H NMR yield (internal standard 1,3,5-trihydroxybenzene) after resin cleavage with TFA/CH<sub>2</sub>Cl<sub>2</sub>. <sup>d</sup> <sup>1</sup>H NMR yield (internal standard 1,3,5-trihydroxybenzene) after resin cleavage with LiBH<sub>4</sub>.

and the subsequent contact of the active species with DCT for at least 2 h prior to the addition of substrates. With minor adaptation, the Crabtree test was applied to the Heck reaction of iodobenzene with *n*-butyl acrylate performed at room temperature. After 15 min, aliquots were taken from the reactions for quantification, and DCT (2 equiv) was added to one reaction vessel. After 24 h, the reactions were stopped for conversion quantification and comparison. The same experimental protocol for the inhibition test was performed with the iodobenzene substrate attached to the Wang resin. It may be argued that the catalytic activity of homogeneous species will be suppressed by DCT and heterogeneous active species will not present any activity in the polymeric matrix. In both cases a partial inhibition of the catalytic activity was observed (Table 2), with only 40% of the original catalytic activity maintained for the free substrate and 50% for the insoluble substrate. The fact that the Heck reaction catalytic activity was in part inhibited by DCT is further strong experimental evidence of the presence of homogeneous catalytically active Pd species.

At this point, the information gathered with poisoning tests cannot be regarded as an unambiguous proof of a homogeneous Heck reaction, and we cannot exclude the participation of palladium colloids or clusters as catalytically active species, as the test range is not known. To gain insight into the reaction mechanism, detailed TEM and UV–vis studies were performed.

**UV–Vis and TEM Studies.** A preliminary study of the Heck reaction of iodobenzene and *n*-butyl acrylate promoted by palladacycle **1** reveals sigmoidal kinetics for the iodobenzene conversion (curve A, Figure 2). It has been found that pretreatment of the palladacycle **1** with *n*-butyl acrylate, NaOAc, and NBu<sub>4</sub>Br for 10 min before the iodobenzene addition cause a pronounced change in the kinetics of the iodobenzene conversion (curve B, Figure 2). The exponential decay observed for the iodobenzene conversion suggests that the palladacycle has been transformed into the catalytically active species during the pretreatment time.

A clearer picture of the hypothesis that catalytically active species are formed in the pretreatment of palladacycle **1** with *n*-butyl acrylate, NaOAc, and NBu<sub>4</sub>Br was provided by UV–vis spectrometry studies. Time-resolved UV–vis was utilized to follow the reaction of palladacycle **1** ( $3.17 \times 10^{-4}$  mol L<sup>-1</sup>) with *n*-butyl acrylate ( $9.5 \times 10^{-3}$  mol L<sup>-1</sup>), NaOAc ( $1.2 \times 10^{-2}$  mol L<sup>-1</sup>), and NBu<sub>4</sub>Br ( $1.6 \times 10^{-3}$  mol L<sup>-1</sup>).

Figure 3 shows the evolution of the absorption band of palladacycle **1** at 360 nm in a reaction time of 30 min. As can

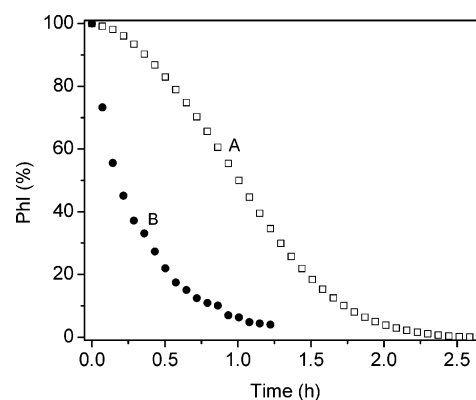


**Figure 2.** Heck reaction of iodobenzene and *n*-butyl acrylate. Reaction conditions: DMA (25 mL), NaOAc ( $0.250 \text{ mol L}^{-1}$ ), *n*-butyl acrylate ( $0.213 \text{ mol L}^{-1}$ ), PhI ( $0.179 \text{ mol L}^{-1}$ ), NBu<sub>4</sub>Br ( $0.035 \text{ mol L}^{-1}$ ), **1** ( $0.179 \text{ mmol L}^{-1}$ ), 80 °C. (□) Reaction performed without pretreatment of the palladacycle. (◆) Reaction performed with pretreatment of the palladacycle **1**.

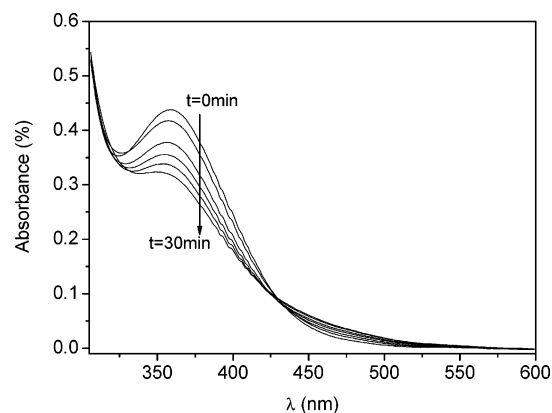


**Figure 3.** Time-resolved UV profile of the palladacycle **1** absorption band with pretreatment time. Reaction conditions: **1** ( $3.17 \times 10^{-4} \text{ mol L}^{-1}$ ), *n*-butyl acrylate ( $9.5 \times 10^{-3} \text{ mol L}^{-1}$ ), NaOAc ( $1.2 \times 10^{-2} \text{ mol L}^{-1}$ ), and NBu<sub>4</sub>Br ( $1 \times 10^{-3} \text{ mol L}^{-1}$ ), RT.

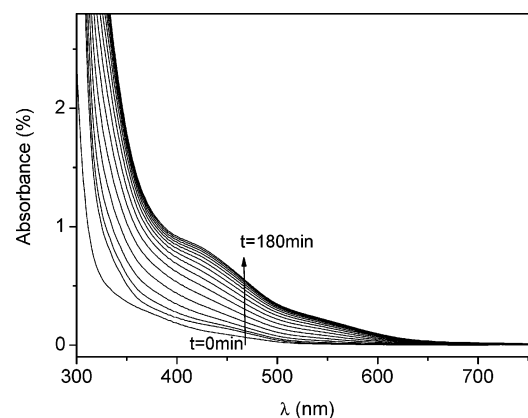


**Figure 4.** Time-resolved UV–vis spectra of the reaction of iodobenzene with *n*-butyl acrylate after a pretreatment time of 40 min. Reaction conditions: **1** ( $3.17 \times 10^{-4} \text{ mol L}^{-1}$ ), *n*-butyl acrylate ( $9.5 \times 10^{-3} \text{ mol L}^{-1}$ ), NaOAc ( $1.2 \times 10^{-2} \text{ mol L}^{-1}$ ), and NBu<sub>4</sub>Br ( $1.6 \times 10^{-3} \text{ mol L}^{-1}$ ), PhI ( $1.2 \times 10^{-1} \text{ mol L}^{-1}$ ), room temperature.

be seen in Figure 3, the gradual decrease of the absorption band at 360 nm is accompanied by a growth in the spectra baseline, possibly related to Pd(0) colloid formation.

After a total pretreatment time of 40 min, iodobenzene ( $1.2 \times 10^{-1} \text{ mol L}^{-1}$ ) was added to the reaction mixture. Figure 4 shows the evolution of a new set of bands with absorption maxima at 540 and 420 nm and a shoulder at 320 nm over a

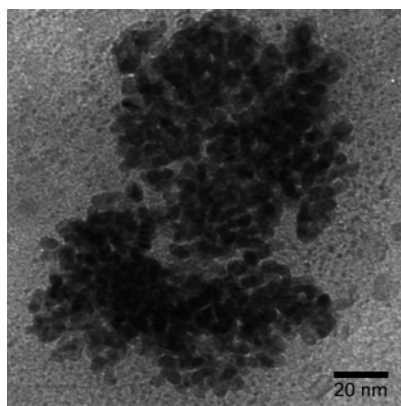


**Figure 5.** TEM micrograph showing the palladium colloids found in the pretreatment solution of palladacycle **1**. Reaction conditions: **1** ( $3.17 \times 10^{-4}$  mol L $^{-1}$ ), *n*-butyl acrylate ( $9.5 \times 10^{-3}$  mol L $^{-1}$ ), NaOAc ( $1.2 \times 10^{-2}$  mol L $^{-1}$ ), and NBu $_4$ Br ( $1.6 \times 10^{-3}$  mol L $^{-1}$ ), room temperature.

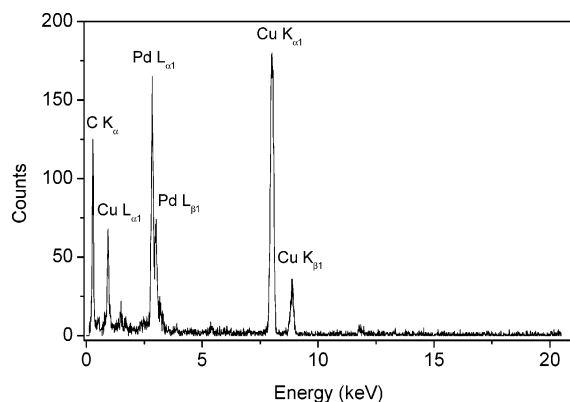


**Figure 6.** EDS analysis of the palladium colloids.

reaction time of 3 h. Although the new species formed cannot be unambiguously assigned, they provide strong evidence for the formation of homogeneous Pd(II) species, regarding the similarity of the bands with those of simple PdX $_n^-$  salts. Thus, these results are in agreement with the process of formation of palladium colloids starting from the palladacycle and the subsequent oxidative addition of the iodoarene on the colloid surface and detachment of the homogeneous Pd(II) species, as pointed out by Reetz.<sup>17b</sup>

The same decrease in the absorption band of palladacycle **1** and appearance of the homogeneous Pd(II) bands were observed in the Heck reaction performed without the pretreatment of the catalytic precursor.

Detailed TEM analysis was performed by withdrawing samples of the reaction before and after iodobenzene addition to the pretreatment solution by simply depositing the solution on carbon-coated copper grids. Palladium colloids were found in the pretreatment solution, as can be seen in the TEM micrograph presented in Figure 5. Palladium colloids were identified by the characteristic palladium lines at 2.83 keV ( $L_{\alpha 1}$ ) and 3.03 keV ( $L_{\beta 1}$ ) in the EDS analysis (Figure 6). After iodobenzene addition, no attempts to identify palladium colloids were successful, indicating that homogeneous species were formed starting from the palladium colloids.

The experimental evidence gathered from the inhibition tests, UV–vis, and TEM studies strongly establishes that palladium colloids are generated starting from palladacycle **1** and they act merely as reservoirs of homogeneous palladium species and the Heck reaction catalytic cycle occurs in the homogeneous phase.

**Kinetic Modeling.** The progress of the Heck reaction of iodobenzene and *n*-butyl acrylate was successfully monitored by time-resolved IR using an ATR probe. The iodobenzene and *trans*-butyl cinnamate concentrations as a function of time were determined by integration of the Ph–I stretching vibration (735 cm $^{-1}$ ) and the out-of-plane deformation at 772 cm $^{-1}$  of the *trans*-butyl cinnamate vinylic hydrogen atoms (Figure 7) employing a response factor determined experimentally by concentration calibration curves. This methodology provides an accurate and noninvasive integral method for the determination of the concentration profile for iodobenzene and the Heck reaction product *trans*-butyl cinnamate during the Heck reaction, since no aliquots are taken from the reaction mixture. Chromatographic analysis of iodobenzene conversion differs from the ATR data no more than 1%.

In our preliminary studies, we tested the ATR methodology to determine the dependence of reaction rates with the concentration of the reaction components at 80 °C using the initial rate method for experimental curves obtained after *pretreatment* of the catalytic precursor (see Supporting Information). We have found a first-order dependence of reaction rate in palladacycle **1** concentration and a zero-order dependence in NaOAc and NBu $_4$ Br concentrations. Interestingly, saturation kinetics was found for both iodobenzene and *n*-butyl acrylate substrates. The existence of an association equilibrium involving olefin coordination to palladium has been reported previously<sup>31</sup> as a highly unfavorable step, and in this case, both iodobenzene and *n*-butyl acrylate can follow saturation kinetics.

On the basis of these data, we propose the Heck reaction mechanism depicted in Figure 8. We assume that, after a pretreatment period of 10 min with NaOAc, NBu $_4$ Br, and *n*-butyl acrylate, the palladacycle **1** is completely converted into the catalytically active Pd(0) species [**1**]. The active species [**1**] can consist of palladium colloids identified by TEM analysis or even highly active forms of low-ligated Pd(0) species stabilized by anions (acetate or halides) and/or solvent molecules, associated with the quaternary ammonium salt. The proposed Heck catalytic cycle is initiated by oxidative addition of iodobenzene to [**1**], followed by the reversible coordination of the olefin ([Acr]) to the oxidative addition product. All the unimolecular subsequent steps (olefin insertion,  $\beta$ -elimination, reductive elimination, and Heck product dissociation) are indistinguishable kinetically and for this reason are combined in a single step characterized by the kinetic constant  $k_3$ .

Using the steady-state approximation for the species [**1**], [**2**], and [**3**], the reaction rate eq 1 can be easily found (for details, see the Supporting Information):

$$-d[\text{PhI}]/dt = \frac{k_1 k_2 k_3 [\text{PhI}][\text{Acr}][\text{Pd}]}{k_2 k_3 [\text{Acr}] + k_1 k_2 [\text{PhI}][\text{Acr}] + k_1 k_3 [\text{PhI}]}$$

The fitting of the reaction rate equation (eq 1) to the experimental curves was performed with the kinetic simulator software Dynafit.<sup>32</sup> The kinetic model depicted in Figure 8 was simultaneously fitted to a set of experimental curves obtained after *pretreatment* of the catalytic precursor showing good agreement with experimental curves. The simulation of the

(31) (a) Rosner, T.; Pfaltz, A.; Blackmond, D. G. *J. Am. Chem. Soc.* **2001**, *123*, 4621. (b) Rosner, T.; Le Bars, J.; Pfaltz, A.; Blackmond, D. G. *J. Am. Chem. Soc.* **2001**, *123*, 1848–1855.

(32) Kuzmic, P. *Anal. Biochem.* **1996**, *237*, 260–273.

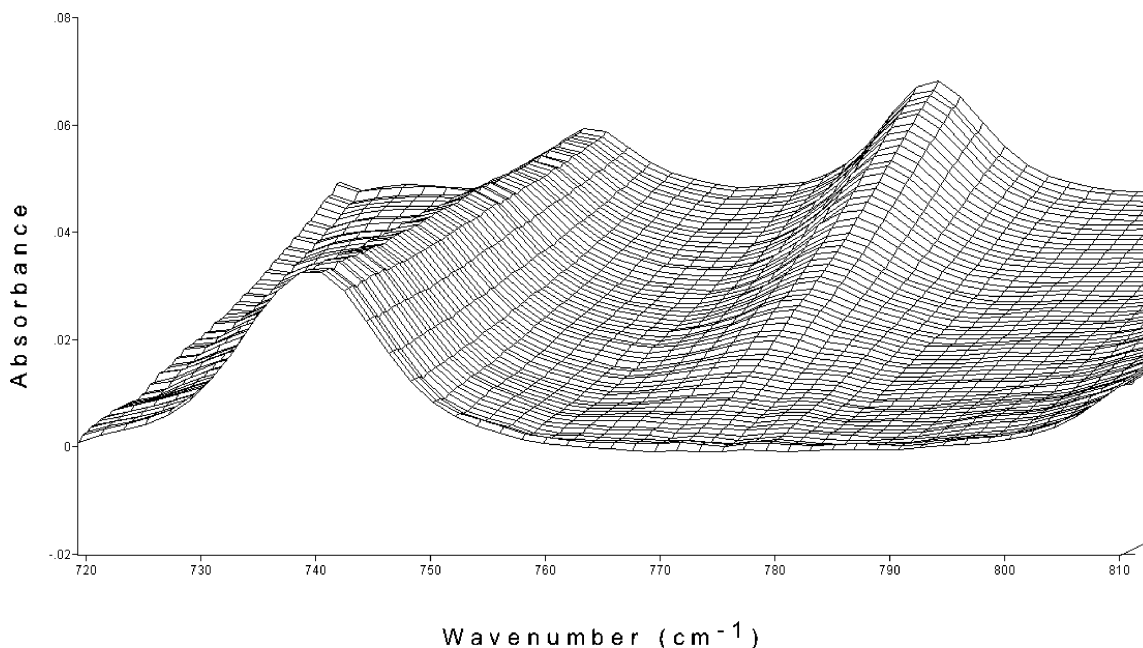


**Figure 7.** Time-resolved ATR-IR showing the C-I stretching vibration ( $735\text{ cm}^{-1}$ ) and *trans*-*n*-butyl cinnamate deformation ( $772\text{ cm}^{-1}$ ) bands versus time during the Heck reaction of iodobenzene and *n*-butyl acrylate promoted by palladacycle **1**. Reaction conditions: DMA (25 mL), NaOAc (0.250 mol  $\text{L}^{-1}$ ), *n*-butyl acrylate (0.213 mol  $\text{L}^{-1}$ ), PhI (0.179 mol  $\text{L}^{-1}$ ),  $\text{NBu}_4\text{Br}$  (0.035 mol  $\text{L}^{-1}$ ), **1** (0.179 mmol  $\text{L}^{-1}$ ),  $80\text{ }^\circ\text{C}$ .

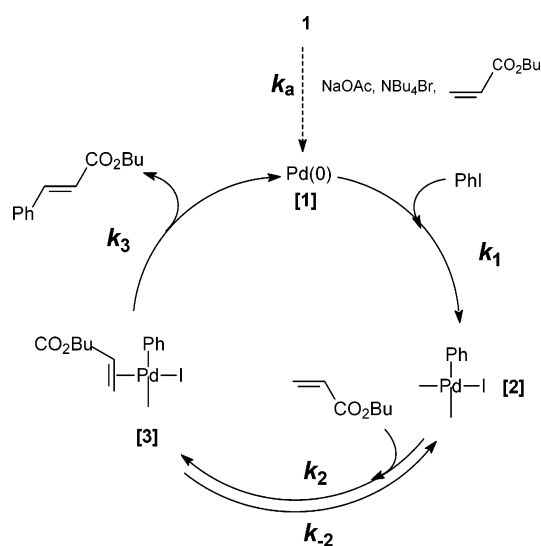


**Figure 8.** Postulated Heck reaction mechanism.

proposed mechanism was performed for reactions starting with three different initial concentrations of *n*-butyl acrylate, iodobenzene, and palladacycle **1**. In this study we avoided artificially low concentrations of *n*-butyl acrylate or iodobenzene, since in the initial rate method we observed a high degree of reaction deactivation. The initial concentrations of the catalytically active species **[1]** after the *preactivation* period were considered to be the same as the palladacycle **1**. The fitting of the model mechanism to experimental data is presented in Figure 9, and the kinetic constants are in Table 3.

It can be seen from the rate constants estimated by the kinetic model that, even with an observed zero-order in iodobenzene concentration over a wide range of initial concentrations employed in this study, the bimolecular oxidative addition step has the highest energy barrier. It is also noteworthy that no simple order in substrate concentration can be derived from eq 1, as the denominator terms in the rate equation cannot be

simplified ( $k_2k_3 = 9375\text{ L mol}^{-1}\text{ s}^{-2}$ ;  $k_1k_3 = 6578\text{ L mol}^{-1}\text{ s}^{-2}$ ;  $k_1k_{-2} = 12\,400\text{ L mol}^{-1}\text{ s}^{-2}$ ). This kinetic model also predicts that relative concentrations of substrate will change the distribution of intermediates involved in the catalytic cycle. A slight excess of alkene relative to iodobenzene leads to a rapid rise in the Pd(0) concentration while when using a slight excess of iodobenzene, relative to alkene, the oxidative addition product is the resting state of the catalytic cycle. This behavior is clearly demonstrated in Figure 10, which shows the concentrations of the palladium intermediates predicted by the rate equation (1) during the Heck reaction starting from different relative substrate concentrations.

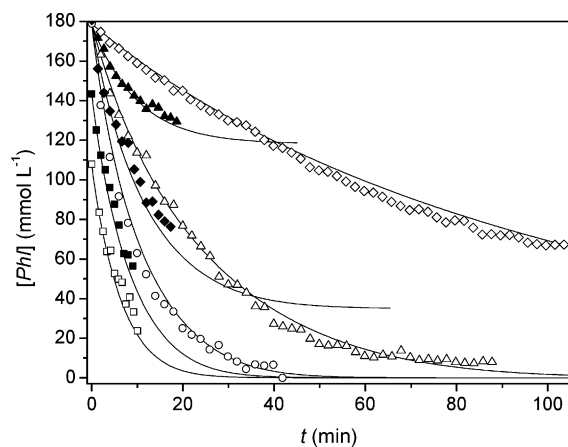
The important conclusion that arises from analysis of this kinetic model is that the initial rate measurements can be highly distorted due to decomposition pathways of the intermediates. In our case we notice palladium black deposition in reactions performed with a *deficiency* of iodobenzene and reaction deactivation by formation of  $\text{PdX}_n^{m-}$  salts via reductive coupling of the oxidative addition product in reactions performed with an *excess* of iodobenzene. The possible deactivation–regeneration pathways involved in the catalytic process are summarized in Figure 11. The first decomposition pathway (deactivation I), i.e., the formation of Pd nanoparticles and eventually Pd metal through agglomeration of Pd(0), has been observed several times.<sup>33,34,35</sup> The agglomeration process is autocatalytic and thermodynamically downhill. In the cases where ligands and/or stabilizing agents are present (exerting a kinetic control on the nucleation step),<sup>36</sup> the regeneration process occurs through oxidative addition of the haloarene to form soluble Pd(II) species (regeneration I). This regeneration process is dependent on halide concentration, and the Pd nucleation rate increases with a decrease in the halide concentration.<sup>37</sup>

(33) Rocaboy, C.; Gladysz, J. A. *New J. Chem.* **2003**, *27*, 39–49.

(34) de Vries, A. H. M.; Mulders, J. M. C. A.; Mommers, J. H. M.; Henderickx, H. J. W.; de Vries, J. G. *Org. Lett.* **2003**, *5*, 3285–3288.

(35) Rocaboy, C.; Gladysz, J. A. *Org. Lett.* **2002**, *4*, 1993–1996.





	[Acr]	[PhI]	[Pd]
△	213	179	0.018
▲	60	179	0.178
◇	213	179	0.08
◆	143	179	0.178
○	213	179	0.178
■	213	143	0.178
□	213	107	0.178

**Figure 9.** Simultaneous fit of eq 1 to experimental curves obtained with different initial concentrations ( $\text{mmol L}^{-1}$ ) of palladacycle **1**, iodobenzene, and *n*-butyl acrylate.

**Table 3.** Rate Constants Determined by Fitting Eq 1 to Experimental Data

constant	fitting	error
$k_1$	$22.3 \text{ L mol}^{-1} \text{ s}^{-1}$	$0.3 \text{ L mol}^{-1} \text{ s}^{-1}$
$k_2$	$33 \text{ L mol}^{-1} \text{ s}^{-1}$	$2 \text{ L mol}^{-1} \text{ s}^{-1}$
$k_{-2}$	$556 \text{ s}^{-1}$	$10 \text{ s}^{-1}$
$k_3$	$295 \text{ s}^{-1}$	$53 \text{ s}^{-1}$

The second decomposition pathway consists of the formation of Pd(II) halide species<sup>34,37,38</sup> (such as  $\text{PdX}_2$ ,  $\text{PdX}_3^-$ ,  $\text{PdX}_4^{2-}$ , and  $\text{Pd}_2\text{X}_6^{2-}$ ) together with the formation of biaryls and haloarene reduction product (deactivation II). These Pd(II) salts and homocoupling and hydrogenolysis products are generated from the oxidative addition intermediate, probably through a bimolecular process.<sup>37</sup> The regeneration (regeneration II) of the catalytically active species occurs through the reduction Pd(II) halides promoted by the base.

The same kinetic model also led to a good fit on reactions performed without the initial pretreatment of the palladacycle **1**. By simply adding a reduction step involving the palladacycle **1** and the additive  $\text{NBu}_4\text{Br}$ , a good agreement with the experimental curve is obtained, as can be seen in Figure 12 with a kinetic constant for precursor reduction of  $k_a = 3.5 \times 10^{-4} \text{ L mmol}^{-1} \text{ s}^{-1}$ .

All attempts to fit the proposed kinetic model into the Heck reaction experimental curves obtained without the pretreatment of the palladacycle **1** failed due to oscillation in the initial induction period with the initial concentrations of NaOAc, *n*-butyl acrylate, and iodobenzene. The only significant effect in reaction rate and induction period was found with different initial concentrations of  $\text{NBu}_4\text{Br}$ , as can be seen in Figure 13.

**The Role of  $\text{NBu}_4\text{Br}$ .** The reaction performed in the absence of the additive  $\text{NBu}_4\text{Br}$  is very slow and occurs with sedimentation of metallic palladium. It is worthwhile noting that for the reactions performed with pretreatment of palladacycle **1** the rates are independent of the salt additive concentration.

This salt effect is much probably related to the role of  $\text{NBu}_4\text{Br}$  as stabilizing agent for the colloidal palladium, which hinders its agglomeration to metallic palladium. Moreover, the “dried”

$\text{NBu}_4\text{Br}$  used in the experiments possibly contains some quantity of  $\text{NBu}_3$  that is responsible for the reduction of Pd(II) salts resulting from the deactivation pathway II (Figure 11). In this respect, it is well-known that at temperatures above  $100^\circ\text{C}$   $\text{NBu}_4\text{Br}$  undergoes partial decomposition with the liberation of  $\text{NBu}_3$ .<sup>39</sup> To check these hypotheses, some experiments were performed using different types of additives (Table 4). It is clear that there are differences between the use of dried and wet  $\text{NBu}_4\text{Br}$  (compare entries 1 and 2, Table 4) on the catalytic performance of palladacycle **1**. This behavior was already observed in Heck coupling reactions promoted by other palladium catalyst precursors.<sup>40</sup> It is also quite fitting that the dried salt additive can be substituted by equal amounts (0.2 equiv) of  $\text{NBu}_3$  (compare entries 1 and 3, Table 4), and in the absence of both salt additive and  $\text{NBu}_3$  only marginal catalytic activities were observed (see entries 2 and 4, Table 4). Note that in the reactions performed with dried  $\text{NBu}_4\text{Br}$ , no deposition of metallic palladium was observed in opposition to those performed in the presence of  $\text{NBu}_3$ , where metallic palladium is formed.

The synergic effect between NaOAc and  $\text{NBu}_3$  combinations can be rationalized in terms of an ideal equilibrium between the deactivation I/regeneration I pathways (Figure 11) involving the catalytically active species.<sup>41</sup> The use of NaOAc alone at lower temperatures promotes the complete deactivation of the system, since the palladium halide species formed during the reaction are not reduced by NaOAc at temperatures below  $130^\circ\text{C}$ . In opposition, the use of sole tertiary amines as base induces the formation of metallic palladium due to their strong and faster reducing properties toward palladium halides species when compared to other bases, such as NaOAc.<sup>41</sup> Therefore for these particular patterns, there are specific relative NaOAc/ $\text{NBu}_3$  concentrations that can generate an ideal equilibrium between the rates of deactivation/regeneration of the Pd catalytically active species, resulting in a higher catalytically active process.

**Aromatic Substituent Effect on Reaction Rate.** The linear free-energy relationship through a Hammett correlation<sup>42</sup> has

(36) Calo, V.; Nacci, A.; Monopoli, A.; Laera, S.; Cioffi, N. *J. Org. Chem.* **2003**, *68*, 2929–2933.  
 (37) Shmidt, A. F.; Khalaika, A. *Kinet. Catal.* **1998**, *39*, 803–807.  
 (38) de Vries, A. H. M.; Parlevliet, F. J.; van de Vondervoort, L. S.; Mommers, J. H. M.; Henderickx, H. J. W.; Walet, M. A. M.; de Vries, J. G. *Adv. Synth. Catal.* **2002**, *344*, 996–1002.

(39) (a) Amiras, M.; Nazeeruddin, M. K.; Grätzel, M. *Thermochimica Acta* **2000**, *348*, 105–114. (b) Prasad, M. R. R.; Krishnamurthy, V. N. *Thermochim. Acta* **1991**, *185*, 1–10.  
 (40) Böhm, V. P. W.; Herrmann, W. A. *Chem. Eur. J.* **2000**, *6*, 1017–1025.  
 (41) Shmidt, A. F.; Khalaika, A.; Bylkova, V. G. *Kinet. Catal.* **1998**, *39*, 194–199.  
 (42) Fuchs, R.; Lewis, E. S. Linear Free-Energy Relations. In *Investigations of Rate and Mechanisms of Reactions*, 4th ed.; Bernasconi, C. F., Ed.; Wiley: New York, 1986, p 777.

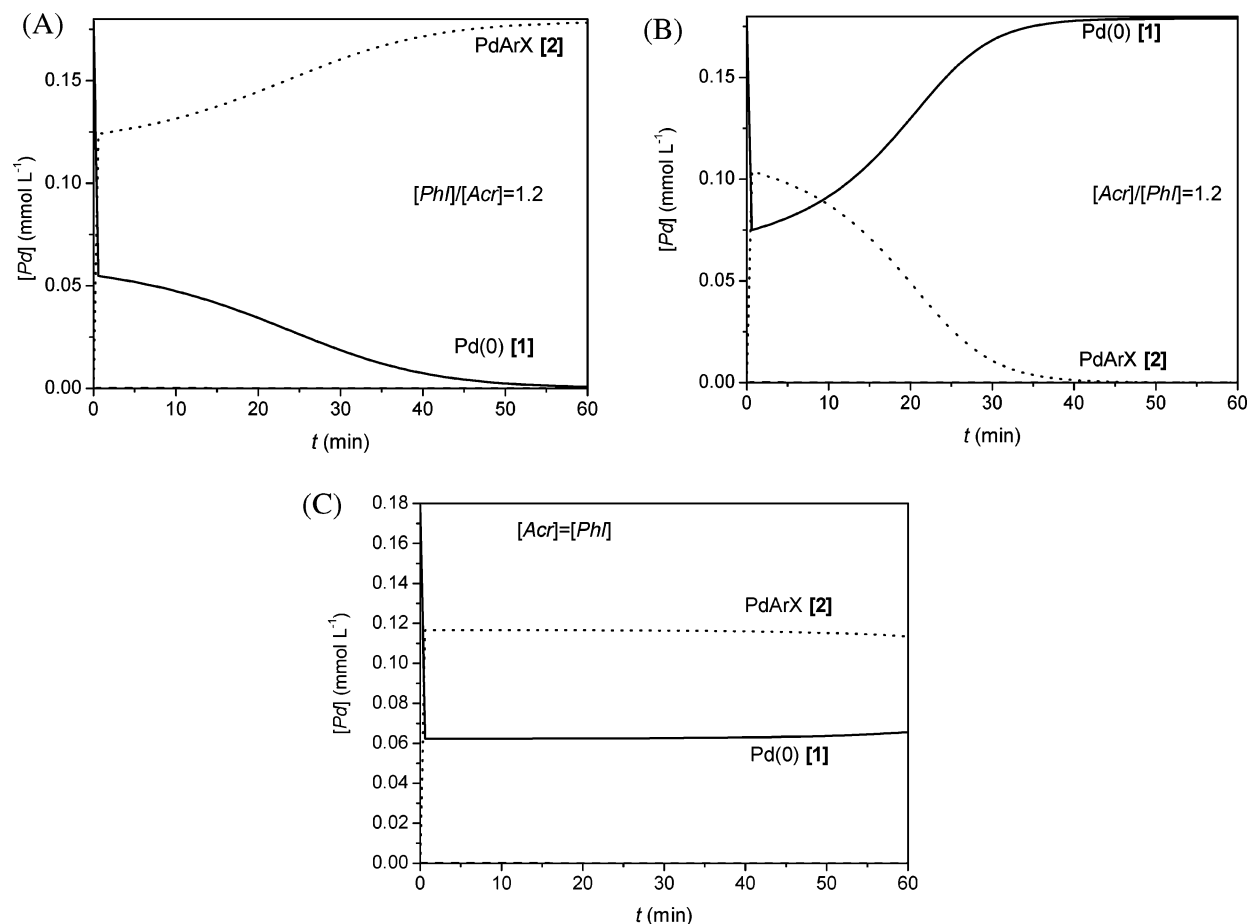


**Figure 10.** Distribution of palladium species within the Heck reaction catalytic cycle using different  $[PhI]/[Acr]$  initial concentration relations.

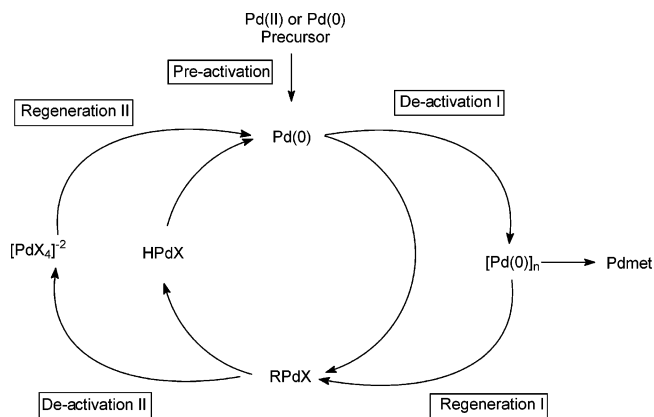


**Figure 11.** Possible deactivation/regeneration of the Pd species involved in the Heck catalytic process.

been used several times to compare the substituent effects of aryl halides in the Heck reaction.<sup>43–47</sup> In most of the cases investigated so far, positive  $\rho$  values were observed, and electron-withdrawing groups are known to increase the rate of the Heck reaction. This electronic effect is more pronounced for chloroarenes than for bromoarenes, followed by iodoarenes. Interestingly, the observed  $\rho$  are on the same order of magnitude, whatever the nature of the Pd catalyst precursor, except in the cases where  $\sigma^-$  was used. However, it is relatively difficult to extract relevant mechanistic information in a multistep reaction sequence, since all of the individual steps involved may affect the final value. Moreover, it is also very difficult to separate

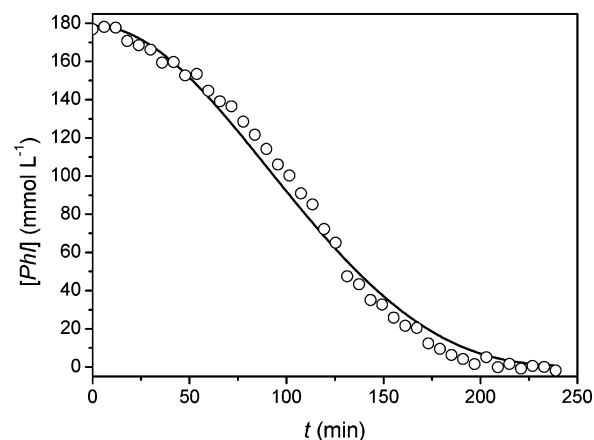


**Figure 12.** Fitting of the kinetic model to the Heck reaction of iodobenzene with *n*-butyl acrylate performed without pretreatment of the palladacycle **1**. Reaction conditions: DMA (25 mL), NaOAc ( $0.250 \text{ mol L}^{-1}$ ), *n*-butyl acrylate ( $0.213 \text{ mol L}^{-1}$ ), PhI ( $0.179 \text{ mol L}^{-1}$ ), NBu<sub>4</sub>Br ( $0.035 \text{ mol L}^{-1}$ ), **1** ( $0.179 \text{ mmol L}^{-1}$ ),  $80^\circ\text{C}$ .

these contributions from each other. Nevertheless, the Hammett correlation is of enormous significance if the differences between the constants obtained for the different catalyst precursors are used for comparison purposes and not their absolute values.

To get more insight into the type of influence that the different substrates may have in a competitive Heck reaction involving differently substituted aryl halides, the kinetic model was extended for two aryl halides (Figure 14). The mechanism is the same as used in the kinetic modeling (Figure 8), except that

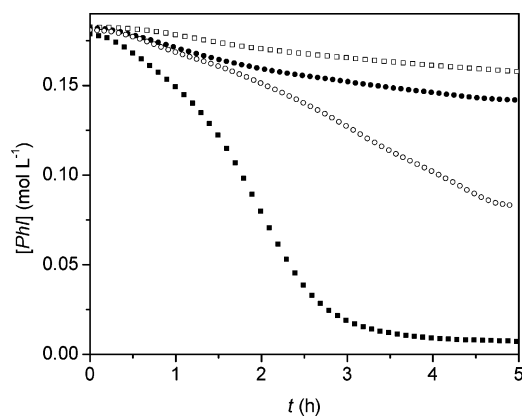


**Figure 13.** Heck reaction of iodobenzene and *n*-butyl acrylate employing different initial  $\text{NBu}_4\text{Br}$  concentrations. Reaction conditions: DMA (25 mL),  $\text{NaOAc}$  ( $0.250 \text{ mol L}^{-1}$ ), *n*-butyl acrylate ( $0.213 \text{ mol L}^{-1}$ ),  $\text{PhI}$  ( $0.179 \text{ mol L}^{-1}$ ), **1** ( $0.179 \text{ mmol L}^{-1}$ ),  $\text{NBu}_4\text{Br}$  (0, 0.017, 0.070, and  $0.13 \text{ mol L}^{-1}$ ),  $80^\circ\text{C}$ .

**Table 4.** Base and Additive Effect in the Heck Reaction between Iodobenzene and *n*-Butyl Acrylate at  $30^\circ\text{C}$  Promoted by Palladacycle **1**<sup>a</sup>

entry	additive	conv (%) <sup>b</sup>	yield (%) <sup>b</sup>
1	dried $\text{NBu}_4\text{Br}$	100	100
2	wet $\text{NBu}_4\text{Br}$	6	6
3	$\text{NBu}_3$	100	100
4	none	10	10

<sup>a</sup> Reaction conditions:  $[\text{PhI}]/[\text{Pd}] = 1.0 \times 10^2$ , 24 h, DMA (5 mL),  $\text{NaOAc}$  (1.4 mmol), *n*-butyl acrylate (1.2 mmol),  $\text{PhI}$  (1 mmol), and additive (0.2 mmol);  $30^\circ\text{C}$ . <sup>b</sup> Yield and conversions determined by GC (methyl benzoate as internal standard).

in this case the reaction starts with the two aryl halides competing for the same catalytically active species **[1]** for the formation of the respective oxidative addition products and the catalytic cycle proceeds with their corresponding rate constants.

The treatment of this mechanism with the steady-state approximation furnishes the following rate equations for the consumption of competing haloarenes:

$$-\text{d}[\text{PhI}]/\text{d}t = \frac{k_1 k_2 k_3 k_2' k_3' [\text{PhI}][\text{Acr}][\text{Pd}]}{a} \quad (2)$$

$$-\text{d}[\text{RPhI}]/\text{d}t = \frac{k_1 k_2 k_3 k_2' k_3' [\text{PhI}][\text{Acr}][\text{Pd}]}{a} \quad (3)$$

$$a = k_2 k_3 k_2' k_3' [\text{Acr}] + k_1 k_2' k_3' [\text{PhI}](k_{-2} + k_3 + k_2 [\text{Acr}]) + k_2' k_3 k_3' [\text{RPhI}](k_{-2}' + k_3' + k_2' [\text{Acr}])$$

The division of eqs 2 and 3 gives eq 4, which expresses the relative reactivity of the two substrates that in its turn is equal to the relative rate of formation of the two different products.

$$\frac{\text{d}[\text{RPhI}]/\text{d}t}{\text{d}[\text{PhI}]/\text{d}t} = \frac{k_1' [\text{RPhI}]}{k_1 [\text{PhI}]} \quad (4)$$

It is now clear that, whatever the rate-limiting step, in a competitive Heck reaction the changes in the relative reactivity involving different aryl halides is strictly bound to the changes

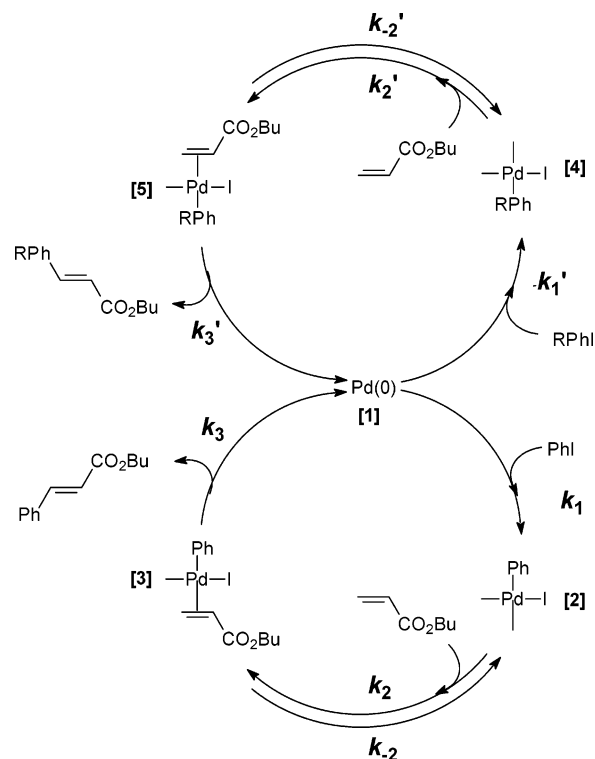


**Figure 14.** Proposed mechanism of a competitive Heck reaction involving two different aryl halides.

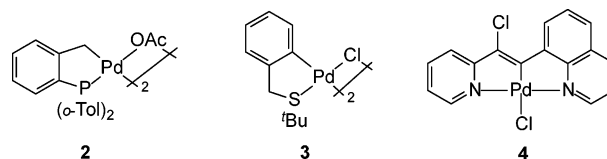


**Figure 15.** Palladacycles used in the Heck competitive experiments.

in the rate constant for the oxidative addition step. According to eq 4 the competitive reactions should be performed under *pseudo-zero-order* conditions relative to the aryl halide (large excess of the aryl halides) or by determining the substrate consumption at very low conversions where the reaction rate does not depend on the aryl halide concentration. Indeed, both assumptions have been corroborated experimentally (see the Supporting Information).

A series of competitive experiments of 4- and 3-substituted iodo- and bromoarenes with *n*-butyl acrylate (iodo- or bromobenzene were used as standards) were performed using palladacycle **1**, and for comparative purposes, the same experiments have been repeated with CP (**2**), CS (**3**), and NCN (**4**) palladacycles (Figure 15).

The reaction was stopped at very low substrate conversions, and the relative rate constants were determined directly using the relative yield obtained by GC. The Hammett parameter was obtained through the slope defined by the straight line that includes the meta-substituents, and the constant ( $\sigma^0$ ,  $\sigma$ , or  $\sigma^-$ ) that best fits the para position was chosen, as recommended for this kind of experiment.<sup>42</sup> The competitive experiments performed between bromo- or iodoarenes with only one substituted aryl halide or with a group of aryl halides that possess similar reactivity (all containing electron-withdrawing or all containing electron-donating groups) gave the same relative reactivity values. Similarly, the same relative reactivity values

**Table 5.**  $R$  and  $r$  Values Obtained in Competitive Heck Experiments Using 3- and 4-Aryl Bromides and Iodides with  $n$ -Butyl Acrylate Promoted by Palladacycles 1–4 Using  $\sigma_0$

palladacycle	X	R	$r$	palladacycle	X	R	$r$
1	Br	0.98	2.5	1	I	0.99	1.8
2	Br	0.98	2.4	2	I	0.98	1.7
3	Br	0.98	2.5	3	I	0.98	1.8
4	Br	0.97	2.5	4	I	0.97	1.8

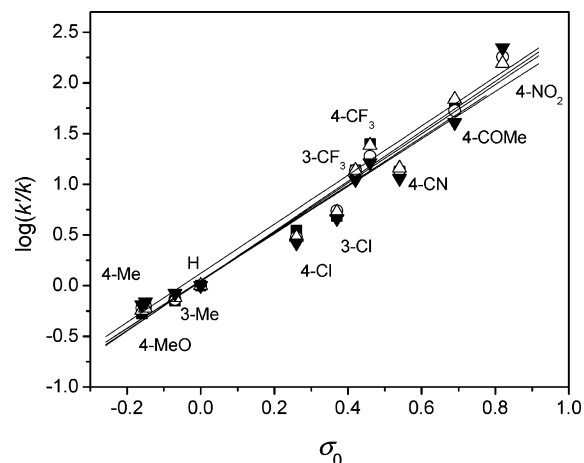


**Figure 16.** Hammett correlation for the competitive Heck reaction between bromoarenes and  $n$ -butyl acrylate at 150 °C in DMA promoted by different palladacycles using the  $\sigma_0$  constants [palladacycles: 1 (○), 2 (▼), 3 (△), 4 (■)].

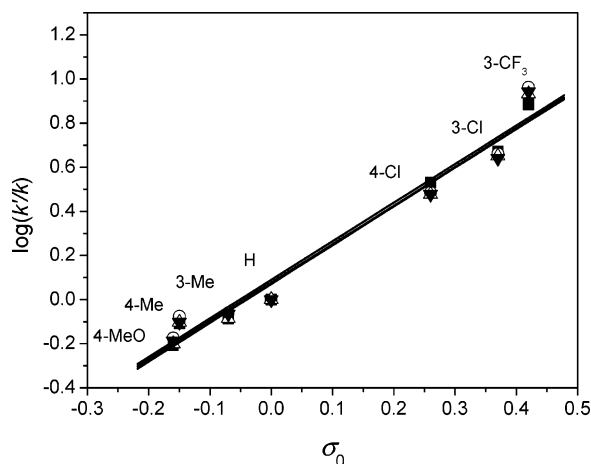


**Figure 17.** Hammett correlation for the Heck competitive reaction between iodoarenes and  $n$ -butyl acrylate at 80 °C in DMA promoted by different palladacycles using the  $\sigma_0$  constants [palladacycles: 1 (○), 2 (▼), 3(△), 4(■)].

were obtained whether the competitive experiments were performed under pseudo-first-order conditions relative to the  $n$ -butyl acrylate or relative to the aryl halides (see Supporting Information).

The use of the  $\sigma_0$  Hammett parameter<sup>42</sup> results in excellent linear correlation (Table 5) for bromoarenes ( $\rho = 2.5$ , Figure 16) and iodoarenes ( $\rho = 1.8$ , Figure 17) for the Heck reaction, indicating that in both cases there is an electronic influence on the reaction rate.

It is also quite impressive that the same  $\rho$  value was obtained (2.4–2.5 for Ar–Br and 1.7–1.8 for Ar–I) for all the four palladacycles, indicating that they form the same active species in the oxidative addition step. The rate of the oxidative addition

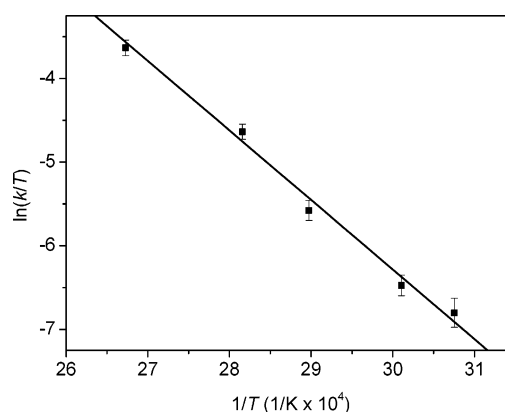


**Figure 18.** Eyring plot for the Heck reaction of iodobenzene and  $n$ -butyl acrylate promoted by palladacycle 1. Reaction conditions: NaOAc (0.250 mol L<sup>-1</sup>), NBu<sub>4</sub>Br (0.035 mol L<sup>-1</sup>),  $n$ -butyl acrylate (21.3 mol L<sup>-1</sup>), PhI (1.78 mol L<sup>-1</sup>), 1 (0.178 mmol L<sup>-1</sup>).  $Y = (18.5 \pm 1.0) + (-8287 \pm 370)X$  ( $R = 0.99$ ).

increases with the presence of electron-withdrawing substituents on the aryl halide, and consequently, the transition state for the oxidative addition is stabilized for groups that remove electronic density from the C<sub>ipso</sub> of the aryl halide. The excellent fit of the slope with  $\sigma_0$  (using the meta-substituents parameters of the aryl halide as standard) shows that there is no formal charge on the transition state of the oxidative step, as suggested by theoretical calculations.<sup>48</sup>

**Activation Parameters.** The activation parameters for the reaction between iodobenzene and  $n$ -butyl acrylate promoted by palladacycle 1 after a pretreatment time of 10 min were determined using the initial reaction rates at different temperatures employing the Eyring equation. The reactions were performed with a large excess of  $n$ -butyl acrylate to ensure first-order kinetics relative to iodobenzene, and consequently the rate law (Equation 1) can be reduced to  $r_i = k_1[\text{PhI}]_0[\text{Pd}]_0$ . The Eyring plot is presented in Figure 18, and the activation parameters  $\Delta H^\ddagger = 69 \pm 3 \text{ kJ mol}^{-1}$  and  $\Delta S^\ddagger = -43 \pm 8 \text{ J mol}^{-1} \text{ K}^{-1}$  could be determined, corresponding to the oxidative addition step if the kinetic model is correct. Indeed, the  $\Delta H^\ddagger$  of  $69 \pm 3 \text{ kJ mol}^{-1}$  is identical to those found for the oxidative addition of iodobenzene with Pd(PPh<sub>3</sub>)<sub>4</sub>.<sup>45,46</sup> Moreover, the entropy of activation of  $-43 \pm 8 \text{ J mol}^{-1} \text{ K}^{-1}$  is consistent with an associative process involving the development of a partial charge in the transition state.

**Conclusions.** The palladacycle {Pd[ $\kappa^1$ -C,  $\kappa^1$ -N-C=C(C<sub>6</sub>H<sub>5</sub>)C(Cl)-CH<sub>2</sub>NMe<sub>2</sub>]( $\mu$ -Cl)}<sub>2</sub>, 1, is merely a reservoir of catalytically active Pd(0) species [1] (Pd colloids or even highly active forms of low-ligated Pd(0) species) that undergoes oxidative addition of the aryl halide on the surface with subsequent detachment of the homogeneous Pd(II) species. The reaction of iodobenzene and  $n$ -butyl acrylate presents a first-order dependence of reaction rate with palladacycle 1 concentration and a zero-order dependence on NaOAc and NBu<sub>4</sub>Br concentrations. Saturation kinetics was found for both iodobenzene and  $n$ -butyl acrylate substrates.

(43) Portnoy, M.; Milstein, D. *Organometallics* **1993**, *12*, 1655–1664.

(44) Ohff, M.; Ohff, A.; Boom, M. E. V. D.; Milstein, D. *J. Am. Chem. Soc.* **1997**, *119*, 11687–11688.

(45) Amatore, C.; Pfluger, F. *Organometallics* **1990**, *9*, 2276–2282.

(46) Fauvarque, J.-F.; Pfluger, F. *J. Organomet. Chem.* **1981**, *208*, 419–427.

(47) Böhm, V. P. W.; Herrmann, W. A. *Chem. Eur. J.* **2001**, *7*, 4191–4197.

(48) (a) Sundermann, A.; Uzan, O.; Martin, J. M. L. *Chem. Eur. J.* **2001**, *7*, 1703–1711. (b) Senn, H. M.; Ziegler, T. *Organometallics* **2004**, *23*, 2980–2988.

The plausible mechanism involves a preactivation step that consists of the complete conversion of **1** into the catalytically active Pd(0) species [**1**]. The main catalytic cycle is initiated by oxidative addition of iodobenzene to [**1**], followed by the reversible coordination of the olefin to the oxidative addition product. All unimolecular subsequent steps (olefin insertion,  $\beta$ -elimination, reductive elimination, and Heck product dissociation) are indistinguishable kinetically and can be combined in a single step. This kinetic model also predicts that a slight excess of alkene relative to iodobenzene leads to a rapid rise in the Pd(0) concentration while when using a slight excess of iodobenzene, relative to alkene, the oxidative addition product is the resting state of the catalytic cycle. The kinetic model extended for a competitive Heck reaction involving two-different aryl halides indicates that, whatever the rate-limiting step, in a competitive Heck reaction, the changes in the relative reactivity involving different aryl halides is strictly bound to the changes in the rate constant of the oxidative addition step. The same  $\rho$  value (2.4–2.5 for Ar–Br and 1.7–1.8 for Ar–I) observed in competitive experiments catalyzed by **1** and CS, CP, and NCN palladacycles suggests that the same active species is involved

in the oxidative addition step. Moreover, the activation enthalpy of  $\Delta H^\ddagger = 69 \pm 3 \text{ kJ mol}^{-1}$  obtained for iodobenzene is identical to those reported for the oxidative addition of iodobenzene with Pd(PPh<sub>3</sub>)<sub>4</sub>. The excellent fit of the slope with the  $\sigma_0$  Hammett parameter and entropy of activation of  $-43 \pm 8 \text{ J mol}^{-1} \text{ K}^{-1}$  is consistent with an associative process involving the development of a partial charge in the transition state (no formal charge) for the oxidative step.

**Acknowledgment.** We thank CNPq, CAPES, and CT-PETRO for partial financial support and a scholarship to C.S.C. We also thank Dr. G. Machado for the TEM analysis and Prof. Dr. G. Eberlin for help in the preparation of DCT.

**Supporting Information Available:** Reaction orders determined by the initial rate method, deduction of rate equations, script used in Dinafit kinetic simulations, typical ATR calibration curve, and Hammett plots obtained with different substrates relative concentrations. This material is available free of charge via the Internet at <http://pubs.acs.org>.

JA051834Q